Journal of Fluorescence (2019) 29:1265–1275
https://doi.org/10.1007/s10895-019-02440-x

ORIGINAL ARTICLE

Synthesis and Crystallographic, Absorption and Emission Studies of 4-Pyridine Carboxamide of Zn(II) 4-Chlorophenylacetate

Füreya Elif Özbek[1] · Mustafa Sertçelik[1] · Mustafa Yüksek[2] · Güventürk Uğurlu[3] · Ali Murat Tonbul[4] · Hacali Necefoğlu[4,5] · Tuncer Hökelek[6]

Received: 27 May 2019 / Accepted: 10 September 2019 / Published online: 23 October 2019

Abstract

A new zinc(II) complex, $[Zn(CB)_2(INA)_2]$ (where CB is 4-chlorophenylacetate and INA is 4-pyridine carboxamide) was synthesized. The structure of the complex was characterized by elemental analysis, FT-IR spectroscopy and single-crystal X-ray diffraction technique. Besides, the thermal stability of the complex was investigated by TGA/DTA analysis method. Moreover, the optical absorption and the emission features of the complex were examined by using UV-Vis and fluorescence spectrophotometers, respectively. Furthermore, Density Functional Theory (DFT) calculations were carried out to support the experimental results. Accordingly, it was determined that the complex crystallized in a monoclinic system with space group P*c*, a = 8.3329 (2) Å, b = 25.6530 (4) Å, c = 13.5048 (3) Å, $\alpha = 90°$, $\beta = 91.703$ (3)° and $\gamma = 90°$. The complex consists two crystallographically independent molecules. In each molecule, the Zn^{II} ion adopts a distorted trigonal pyramidal coordination formed by two O atoms from the two 4 chlorophenylacetate ligand and two N atoms of the two 4-pyridine carboxamide ligands. It was observed that the linear absorption spectra of the complex were similar to linear absorption spectra of the semiconductors. In addition, two emission peaks were observed in the fluorescence spectra which could be due to the formation of excimer and the interactions of the benzene and pyridine rings. The energy gap ($\Delta E_{gap} = E_{LUMO} - E_{HOMO}$) of the complex has been calculated as 3.712 eV and this value is very close to the experimentally measured value (3.86 eV). Therefore, because of higher fluorescence intensity of emission peak that was observed between 309 and 556 nm wavelength besides other traits, the complex could potentially be used in the blue light OLED application by filtering of the emission peak around 710 nm wavelength.

Keywords Zn complex · 4-Chlorophenylacetic acid · Optical absorption · Fluorescence · DFT

Electronic supplementary material The online version of this article (https://doi.org/10.1007/s10895-019-02440-x) contains supplementary material, which is available to authorized users.

✉ Füreya Elif Özbek
fozturkkan36@gmail.com

[1] Department of Chemical Engineering, Kafkas University, 36100 Kars, Turkey

[2] Department of Electrical and Electronic Engineering, Kafkas University, 36100 Kars, Turkey

[3] Department of Physics, Kafkas University, 36100 Kars, Turkey

[4] Department of Chemistry, Kafkas University, 36100 Kars, Turkey

[5] International Scientific Research Centre, Baku State University, 1148 Baku, Azerbaijan

[6] Department of Physics, Hacettepe University, 06800 Beytepe, Ankara, Turkey

Introduction

Scientists have spent much effort in coordination chemistry for more than a century to synthesis new complexes with transition metals for fluorescence [1–3], catalysis [4–6], electrochemistry [7], antibacterial [8, 9], chemical sensors [10, 11], electronic devices [12–14], nonlinear optic [15–17] and gas adsorption [18] applications. The complexes which are exhibited fluorescence behavior have a wide application area such as: (i) protein detecting with high sensitivity [14], (ii) nitroaromatic explosive detecting [19], (iii) DNA sequencing [20]. The purpose of the crystal engineering is to explore new materials with particular interest which can be used in various application areas. In this context, the structures, biological and physical properties of the complexes are affected by metal ions, ligands in the coordination, and intermolecular interactions. When these intermolecular interactions are examined, it

has been determined that the structure is affected by weak forces despite the strong forces in action [21, 22].

Carboxylate ligands are widely used in the construction of mixed ligands complexes due to their ability to exhibit various coordination modes [23]. Flexible carboxylic acids with C − O − M − O cyclic mode are the ideal ligands for the construction of new coordination compounds with central metal ions, increasing the stability of transition metal complexes [24]. One of these flexible ligands is phenylacetic acid. Some metal complexes of phenylacetic acid and its derivatives consisting of fluoro, chloro, methoxy, hydroxyl and nitro groups are known [24–28]. The 4-chlorophenylacic acid, which is a derivative of phenylacetic acid, which we use in our study, has a carboxylate group that can be used as a versatile binder. However, so far, there are a few studies on the metal complexes of 4-chlorophenylacetic acid [25, 29]. In the structure of these complexes, there are also some auxiliary ligands. The N-, O-, S- donor heteroaromatic ligands are good candidates for the design and synthesis of different crystal architectures. The 4-pyridine carboxamide which is known as isonicotinamide (INA), is an important N- and O- donor ligand. There are 24 complexes transition metal arylcarboxylate with isonicotinamide complexes whose crystal structure has been examined. Half of these complexes exhibit a monomeric structure, three of which are dimeric structure and three of which are polimeric structure. 4-pyridine carboxamide has two potential donor sites: the nitrogen atom of pyridine ring and the carboxamide oxygen atom. Except for one complex, among all its complexes, 4-pyridine carboxamide acts as a monodentate ligand in which the nitrogen atom of pyridine ring is coordinated with the metal ions. In addition, there is an only complex in which 4-pyridine carboxamide is coordinated as bidentate and there are also several complexes that are ionic [30–32].

In light of these assessments, we chose the 4-Chlorophenylacetic acid as an O-donor candidate and 4-pyridine carboxamide ligand as an interesting N-donor candidate to create the $[Zn(4\text{-}CB)_2(INA)_2]$ complex. We are reporting the crystal structure, thermal behavior, optic and fluorescence properties of this complex.

Materials and Methods

All reagents and solvents reactive grade chemicals were purchased commercially and used without any purification. Micro analytical (C, H and N) data were obtained with the LECO, CHNS-932 elemental analyzer. FT-IR spectra were recorded with a Perkin Elmer Frontier™ FT-IR Spectrometer in the region 4000–600 cm^{-1} using ATR method. TGA was carried out with a Schimadzu DTG 60 thermal analyzer (in N_2 atmosphere; the temperature range: 25–1000 °C; the heating rate: 10 °C min^{-1}; the reference material: highly sintered α-Al_2O_3). The complex was dissolved in dimethylformamide (DMF) solution at 0.05 g/mL concentration [33]. The linear absorption characteristics of the complex were measured by UV-Vis spectrophotometer (Shimadzu UV-1800) at room temperature. The emission measurements of the complex were recorded by fluorescence spectrophotometer (Perkin Elmer LS55). The complex was excited with a lot of excitation wavelengths among 200 nm and 700 nm. But the maximum emission intensity was obtained under 200 nm excitation wavelength.

Preparation of bis(4-chlorophenylacetate) bis(4-pyridine carboxamide)zinc(II)

In order to prepare sodium 4-chlorophenylacetate, 0.84 g (10 mmol) $NaHCO_3$ and 1.71 g (10 mmol) 4-chlorophenylacetic acid were mixed in 100 mL distilled water and the solution was stirred and heated up to 60 °C which CO_2 gase was completely removed. Then, in another beaker, 0.89 g

Table 1 Experimental details for complex

Empirical formula	$C_{28}H_{24}Cl_2N_4O_6Zn$
Formula weight	648.80
Colour/shape	colourless/prism
Temperature (K)	293(2)
Wavelenght (Å)	0.71073
Crystal System	monoclinic
Space Group	*Pc*
a (Å)	8.3329 (2)
b (Å)	25.6530 (4)
c (Å)	13.5048 (3)
α (°)	90
β (°)	91.703 (3)
γ (°)	90
V (Å^3)	2885.56 (10)
Z	2
μ (Mo K_α) (mm^{-1})	1.09
ρ (calcd) (mg m^{-3})	1.493
Number of Reflections Total	27,799
Number of Reflections Unique	10,952
R_{int}	0.059
$2\theta_{max}$ (°)	52.8
T_{min} / T_{max}	0.574 / 0.745
Number of Parameters	740
GOF	1.19
R [$F^2 > 2\sigma(F^2)$]	0.064
wR	0.144
$(\Delta\rho)_{max}$ (e Å^{-3})	0.38
$(\Delta\rho)_{min}$ (e Å^{-3})	−0.50

(5 mmol) $ZnSO_4.H_2O$ and 1.22 g (10 mmol) 4-pyridine carboxamide were dissolved in 20 mL distilled water. 4-pyridine carboxamide and sodium 4-chlorophenylacetate solutions were added on $ZnSO_4.H_2O$ solution, respectively. The obtained colorless crystals were filtered off and washed with distilled water. The crystals were dried at room temperature [34].

Yield 2.46 g (76%). Anal. Calcd. (%) for the Complex, $C_{28}H_{24}Cl_2N_4O_6Zn$ (MW = 648.80 g/mol) C, 51.83; H, 3.73; N, 8.64. Found: C, 47.24; H, 3.13; N, 8.82.

X-ray Crystallography

Single-crystal X-ray diffraction analysis of the obtained complex was performed on a Bruker APEX-II CCD diffractometer. Structure was solved by direct methods and refined by full-matrix least squares against F^2 using SHELXS-97 [35]. All non-H atoms were refined anisotropically. The N- and C-bound H atoms were positioned geometrically at distances of 0.86 Å (NH), 0.93 Å (for CH) and 0.97 Å (for CH_2) from the parent N and C atoms; a riding model was used during the refinement processes and the U_{iso} (H) values were constrained to be $1.2U_{eq}$ (carrier atom). Experimental details are given in Table 1.

Theoretical Method

The molecular geometry optimization of crystal structure was performed by the DFT method employing Becke's three parameter hybrid functional (B3) and combined with gradient corrected correlation functional of Lee–Yang–Parr (LYP) [36, 37] and employing Los Alamos National Laboratory 2-Double-Zeta (LanL2DZ) basis set [38]. After optimization, the vibrational frequency, polarizability (α), the hyperpolarizability (β), highest occupied molecular orbital (HOMO) and the lowest unoccupied molecular orbital (LUMO) values have been calculated at B3LYP/6-31G level of theory. Gaussian 09 program package and Gauss view 5.0 molecular visualization program were used for all of the calculations [39, 40].

Table 3 Hydrogen-bond geometry for the complex (Å, °)

D-H···A	D-H	H···A	D···A	D-H···A
N2—H2C···O12^{i}	0.86	2.16	2.995 (8)	163
N2—H2D···O1^{ii}	0.86	2.11	2.956 (9)	167
N4—H4C···O4^{iii}	0.86	2.44	3.089 (8)	133
N4—H4D···O3^{iv}	0.86	2.10	2.922 (9)	161
N6—H6C···O8^{v}	0.86	2.04	2.871 (8)	163
N6—H6D···O7^{ii}	0.86	1.98	2.807 (8)	160
N8—H8C···O5^{vi}	0.86	2.22	3.031 (8)	158
N8—H8D···O9^{iv}	0.86	2.12	2.968 (9)	169
C20—H20···O1^{ii}	0.93	2.33	3.191 (8)	154
C21—H21···O6^{vii}	0.93	2.43	3.309 (9)	158
C26—H26···O3^{iv}	0.93	2.43	3.348 (8)	169
C27—H27···O6^{viii}	0.93	2.33	3.158 (9)	149
C41—H41···Cl2^{iii}	0.93	2.76	3.556 (11)	144
C48—H48···O7^{ii}	0.93	2.44	3.336 (8)	163
C49—H49···O11^{ix}	0.93	2.23	2.993 (9)	139
C54—H54···O9^{iv}	0.93	2.35	3.180 (9)	148
C7—H7···Cg5^{ix}	0.93	2.58	3.468 (11)	159

Table 2 Selected bond lengths (Å) and angles (°) for the complex

Molecule I		Molecule II		
	Experimental		Experimental	DFT
Zn1—O2	1.949 (5)	Zn2—O8	1.956 (5)	1.9710
Zn1—O4	1.984 (5)	Zn2—O10	1.943 (6)	1.9857
Zn1—N1	2.046 (5)	Zn2—N5	2.045 (5)	2.0992
Zn1—N3	2.026 (5)	Zn2—N7	2.011 (6)	21,152
O1—C1	1.217 (9)	O7—C29	1.204 (9)	1.2681
O2—C1	1.289 (9)	O8—C29	1.285 (9)	1.3157
O3—C9	1.211 (8)	O9—C37	1.236 (9)	1.2776
O4—C9	1.273 (8)	O10—C37	1.270 (9)	1.3229
O2—Zn1—O4	95.0 (2)	O8—Zn2—N5	102.8 (2)	104.5
O2—Zn1—N1	110.0 (2)	O8—Zn2—N7	115.4 (2)	106.5
O2—Zn1—N3	114.6 (2)	O10—Zn2—O8	96.8 (2)	98.8
O4—Zn1—N1	120.5 (2)	O10—Zn2—N5	114.3 (2)	113.2
O4—Zn1—N3	104.2 (2)	O10—Zn2—N7	114.1 (3)	110.8
N3—Zn1—N1	111.7 (2)	N7—Zn2—N5	112.0 (2)	111.9
O1—C1—O2	122.9 (7)	O7—C29—O8	122.3 (8)	124.4
O3—C9—O4	121.6 (6)	O9—C37—O10	122.8 (8)	121.9

Result and Discussion

Crystal Structures of the Complex

The X-ray structural analyses of the complex confirm the assignment of its structure from spectroscopic data. Obtained experimental and theoretical bond lengths and angles are given in Table 2. For bond lengths and angles, there is a good agreement between obtained values from single crystal X-ray and DFT studies. Hydrogen bond geometry is given in Table 3. The molecular structure along with the atom-numbering scheme is depicted in Fig. 1, while the parial packing diagram is given in Fig. 2.

The asymmetric unit of the crystal structure of the mononuclear complex contains two crystallographically independent molecules, where the metal atoms, Zn1 and/or Zn2, are coordinated by two 4-chlorophenylacetate (CB) anions and two 4-pyridine carboxamide (INA) ligands coordinating in a monodentate manner (Fig. 1). The Zn^{II} cations are tetra-coordinated via two nitrogen atoms of INA and two oxygen atoms of CB anions. The two carboxylate O atoms of the monodentate CB anions and the two N atoms of the INA ligands form a distorted trigonal pyramidal coordination sphere around the Zn atoms. The average Zn—O and Zn—N bond lengths are [1.967(5) Å and 2.036(5) Å (for molecule I)] and [1.950(6) Å and 2.028(6) Å (for molecule II)], respectively, while the average O—Zn—N bond angles are [112.3(2)° (for molecule I)] and [111.7(2)° (for molecule II)] (Table 2). On the other hand, the O—Zn—O and N—Zn—N bond angles are [95.0(2)° and 111.7(2)° (for molecule I)] and [96.8(2)° and 112.0(2)° (for molecule II)], respectively (Table 2). The near equalities of the {O1—C1[1.217(9) Å], O2—C1[1.289(9) Å], O3—C9[1.211 (8) Å], O4—C9[1.273(8) Å])° (for molecule I)} and {O7—C29 [1.204(9) Å], O8—C29 [1.285(9) Å], O9—C37 [1.236(9) Å], O10—C37 [1.270(9) Å])° (for molecule II)} bonds in the carboxylate groups indicate delocalized bonding arrangements rather than localized single and double bonds. The {O1—C1—O2 [122.9(7)°], O3—C9—O4 [121.6(6)°])° (for molecule I)} and {O7—C29—O8 [122.3(8)°], O9—C37—O10 [122.8(8)°])° (for molecule II)} bond angles may be compared with the corresponding value present in a free acid [122.2°]. The Zn1 atom lies 0.0645(7) Å below and 0.2267(6) Å above of the planar (O1/O2/C1) and (O3/O4/C9) carboxylate groups, respectively, while Zn2 atom lies 0.5586(6) Å below and 0.0101(7) Å above of the planar (O7/O8/C29) and (O9/O10/C37) carboxylate groups, respectively. In the CB anions, the carboxylate [(O1/O2/C1) and (O3/O4/C9)] groups are

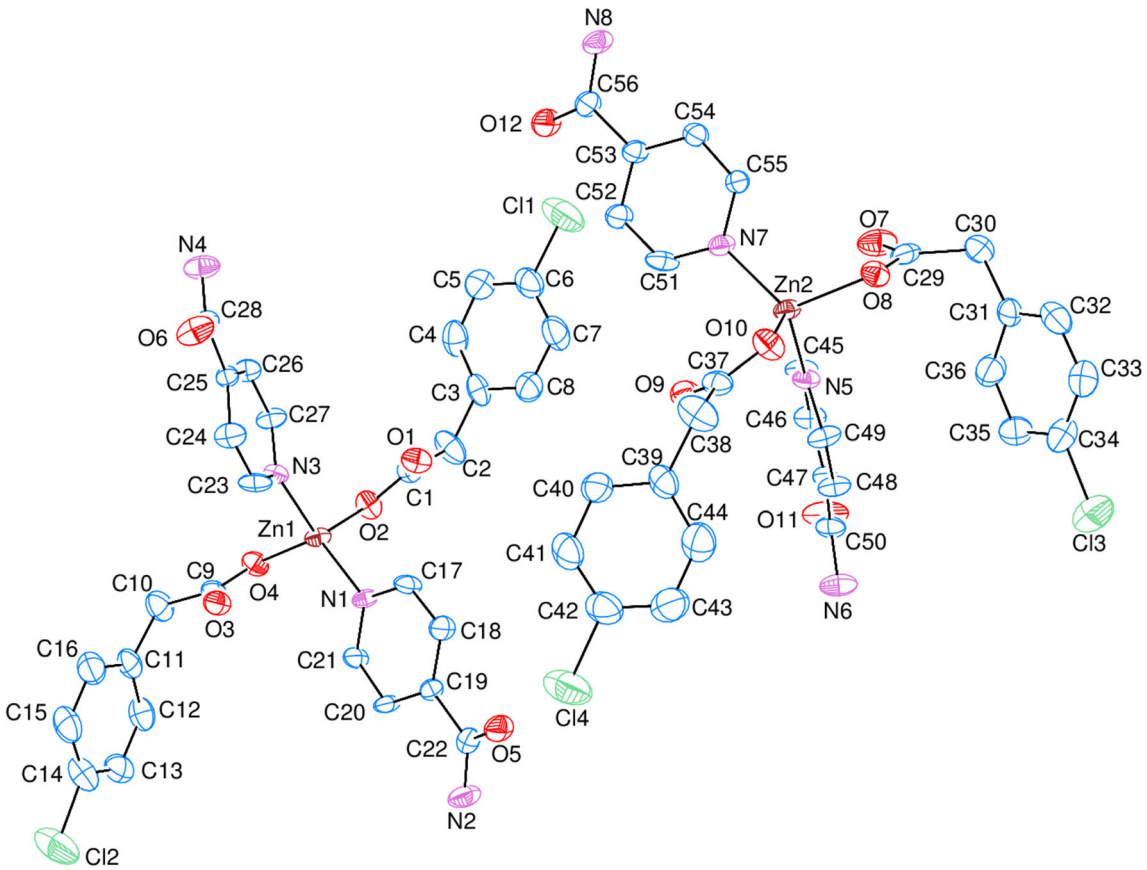

Fig. 1 An ORTEP-3 view of the complex. The thermal ellipsoids are drawn at the 30% probability level. Hydrogen atoms have been omitted for clarity [49]

twisted away from the attached benzene [*A* (C3—C8) and *B* (C11—C16)] rings by 70.3(5)° and 70.1(6)°, respectively, while the carboxylate [(O7/O8/C29) and (O9/O10/C37)] groups are twisted away from the attached benzene [*E* (C31—C36) and *F* (C39—C44)] rings by 79.8(7)° and 65.2(7)°, respectively. The pyridine [*C* (N1/C17—C21), *D* (N3/C23—C27)] and pyridine [*G* (N5/C45—C49), *H* (N7/C51—C55)] rings are oriented at dihedral angles of [*A*/*B* = 86.8(2)°, *A*/*C* = 9.4(3)°, *A*/*D* = 75.3(2)°, *B*/*C* = 78.3(2)°, *B*/*D* = 23.0(3)°, *C*/*D* = 65.9(2)°] and [*E*/*F* = 37.3(3)°, *E*/*G* = 34.1(2)°, *E*/*H* = 34.1(2)°, *F*/*G* = 71.4(3)°, *F*/*H* = 3.2(3)°, *G*/*H* = 68.2(2)°].

In the crystal structure, NH_2 groups link to the carboxylate and INA oxygen atoms via intermolecular N—H···O hydrogen bonds (Table 3) through the $R_2^2(8)$ ring motifs [41] (Fig. 2), while both of the N—H···O and C—H···O hydrogen bonds (Table 3) link the molecules into a supramolecular structure. The π···π interactions between the benzene [*A* (C3—C8) and *F* (C39—C44)] and pyridine [*C* (N1/C17—C21) and *H* (N7/C51—C55)] rings, Cg3—$Cg1^{i}$ and Cg8—$Cg6^{ii}$ [symmetry codes: (i) x - 1, y, z, (ii) x + 1, y, z, where Cg1, Cg3, Cg6 and Cg8 are the centroids of the rings *A* (C3—C8), *C* (N1/C17—C21), *F* (C39—C44) and *H* (N7/C51—C55), respectively] may further stabilize the structure with the centroid-centroid distances of 3.815(5) Å and 3.735(5) Å, respectively. There is also a weak C—H··· π interaction (Table 3).

FT-IR Spectra

The found absorption bands of the experimental and theoretical IR spectra have been given in Table 4. In the IR spectra of the complex, two absorption bands were appeared around 3313 cm^{-1} and 3107 cm^{-1}. These absorption bands can be attributed to the $\nu_{as}(NH_2)$ and $\nu_s(NH_2)$ stretching vibration of N-H bond of 4-pyridine carboxamide, respectively [42]. These stretching vibrations were obtained among 3500–3300 cm^{-1} with help of B3LYP-6-31G calculations. The stretching vibrations related to the methylene group (CH_2) of the CB appeared around 3000 cm^{-1}. The mentioned peak computed at 2991 cm^{-1}. The FT-IR spectroscopy provides useful information about the coordination type of the carboxylate ion. Asymmetric and symmetric vibrations of the COO^- moiety have been showed at 1583 cm^{-1} and 1375 cm^{-1}, respectively. The $\Delta\nu(COO^-)$ value of the complex is calculated from difference between asymmetric and symmetric vibrations of the COO^- group. This value was found to be 209 cm^{-1} for the synthesized complex. Under light on this information, the coordination type of the carboxylate group was determined as monodentate and the X-ray diffraction result confirmed the calculation [25, 29, 43]. Asymmetric and symmetric vibrations of the COO^- vibrations were found at 1560 cm^{-1} and 1337 cm^{-1} for B3LYP-6-31G (Supplemental Figs. 1 and 2).

Thermal Analysis

Thermal Analysis results showed that the complex was stable in the temperature range of 25–125 °C. The complex started to decomposition from 125 °C. In the temperature range of 125–330 °C, INA ligands released (calc.36.60%; exp.34.80%) and accompanied by an exothermic heat effect at 226 °C and 277 °C. In the ongoing decomposition step, the other organic ligands (CB) removed from the structure of the complex. The final product of thermal decomposition was ZnO (calc.87.78%; exp.86.65%) (Supplemental Fig.3).

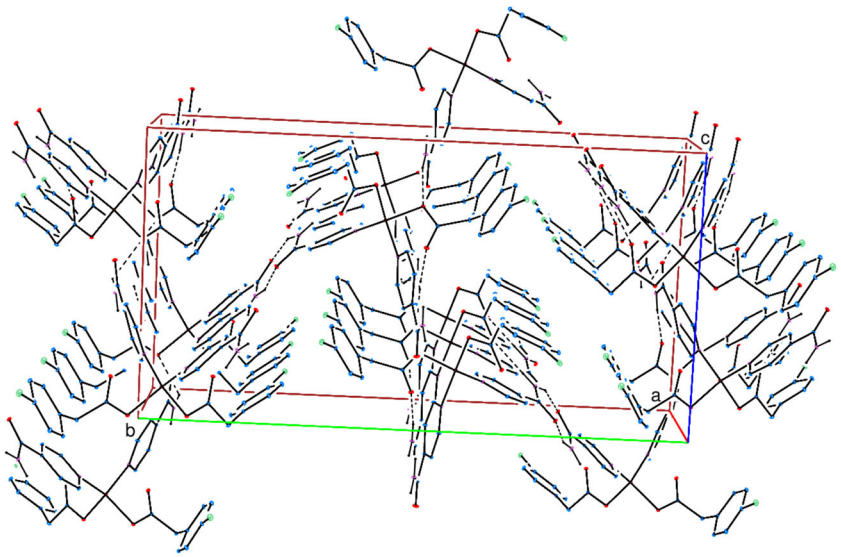

Fig. 2 A partial packing diagram of the complex viewed down the a-axis. Only N—H···O hydrogen bonds are shown as dashed lines. The other H atoms have been omitted for clarity

Table 4 The experimental and theoretical FT-IR spectra of the complex

Assignment	Experimental	Theoretical
ν(N-H)$_{as}$, ν(N-H)$_{s}$,	3313w, 3107w	3494, 3307
ν_{ar}(C-H)	3007w	3087
ν_{aliph}(C-H)	2960w, 2910 w	3000, 2938
ν(C=O)	1689s	1632
δ(N-H)	1617s	1670
ν(C=C)	1490 m	–
$\nu(COO^{-})_{as}$	1547s	1560
$\nu(COO^{-})_{s}$	1375s	1337
$\Delta(COO^{-})$	199	223
ν(C-O)	1375s	1360
$\nu(CN^{-})_{py}$	1283 m	1266
ν(C-Cl)	856 m	854
ν(Me-O)	654 s	678

Molecular Electrostatic Potential (MEP)

The three-dimensional (3D) molecular electrostatic potential (MEP) surface map is showing the electron density of the molecule. The value of MEP, V(r), constituted by molecule system at any point, r(x, y, z), gives the electrostatic energy on the unit positive charge position r(x, y, z). The Calculated 3D plot of MEP for the complex has been shown in Fig. 3. The electrostatic energy values ranges from -8.156×10^{-2} a.u. to $+8.156 \times 10^{-2}$ a.u. The red, blue and green colors, taking place in the Fig. 3 indicate the negative, positive and zero potentials, respectively. The negative and positive potentials are consisted of the oxygen atoms of carbonyl groups and hydrogen atoms of amino groups, respectively. On the other hand, chlorine atoms bonded to the benzene rings lead to smaller negative potential (orange or yellow color) according to the oxygen atoms of carbonyl groups.

HOMO-LUMO Analysis

HOMO (Highest Occupied Molecular Orbitals) and LUMO (Lowest Unoccupied Molecular Orbitals) energies of the complex were calculated by B3LYP/6-31G method and the results have been given in Table 5. The 3D plots of both of highest occupied and lowest unoccupied molecular orbitals of the complex are shown in Fig. 4. The determination of the HOMO and LUMO orbitals are extremely significant for the optic and optoelectronic applications. The energy gap which was taken place between HOMO and LUMO orbitals of the complex found to be 3.712 eV and this value close to the experimentally found value (3.86 eV). In addition, the experimental and theoretical energy gaps values of the complex were found to be compatible with the energy gap of Zn (II) bis(3,4-dimethoxybenzoate)bis(nicotinamide) dihydrate in the literature [44].The determination of the HOMO and LUMO energies as negative demonstrate the stability of the complex [45].

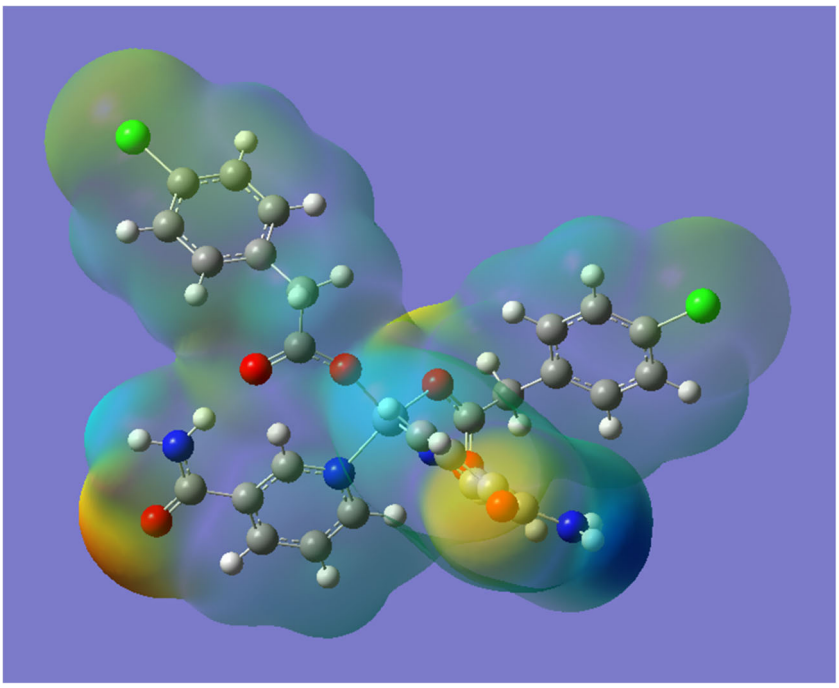

Fig. 3 3D MEP illustration of the complex obtained from (B3LYP/6-31G) calculation

Linear Absorption and Emission Behaviors

The linear absorption spectra help to determine the optical application of the materials. The measured linear optical spectra of the complex are given in Fig. 5. As seen from the figure, the complex has absorption spectra which are similar to the linear absorption spectra of the semiconductors [46]. That is, the spectra where there is no linear absorption in a certain region, but there is a sharp increase at the absorption edge in one place. The sharp increment of the linear absorption of the complex started from 321 nm wavelength and this corresponds to nearly 3.86 eV in energy. The electron transitions which are cause to the linear absorption behaviors in the organic complexes can be shown schematically as in Fig. 6. Related to the Fig. 6, the $n \rightarrow \pi^*$ and $\sigma \rightarrow \sigma^*$ electronic transitions are contributing to the linear absorption spectra of the complex.

The emission (fluorescence) spectra of the Zn(II) complex has been shown in the inset of the Fig. 6. Unlike previous studies [47–51] which are done upon the investigation of the complexes with Zn(II), we observed two emission peaks. The $\pi^* \rightarrow n$ and $n \rightarrow \pi$ emissions lead to fluorescence peak among 309–556 nm. These emissions are mainly causing from the relaxations of the electrons between the upper and lower electronic states of Zn^{II} cation. When compared the emission intensity of Zn^{II} with the literature, here we found larger fluorescence intensity according to previous studies [33, 52, 53]. On the other hand, formation of excimer [54, 55] and interactions of the benzene and pyridine rings with each other are contributing to a emission peak among 630–843 nm wavelengths. These behaviors are supported by the our single crystal X-ray diffraction results (Figs. 1 and 2) [34].

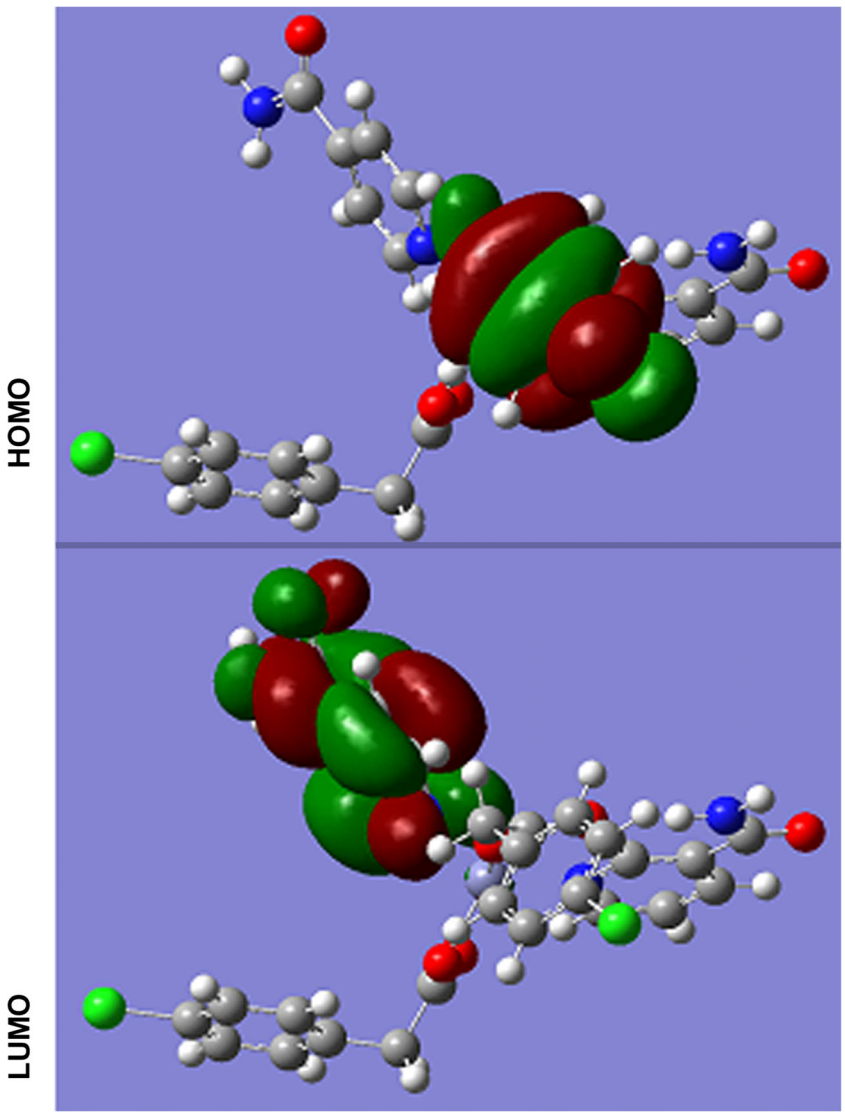

Fig. 4 3D HOMO and LUMO plots of the complex obtained from the (B3LYP/6-31G) calculations

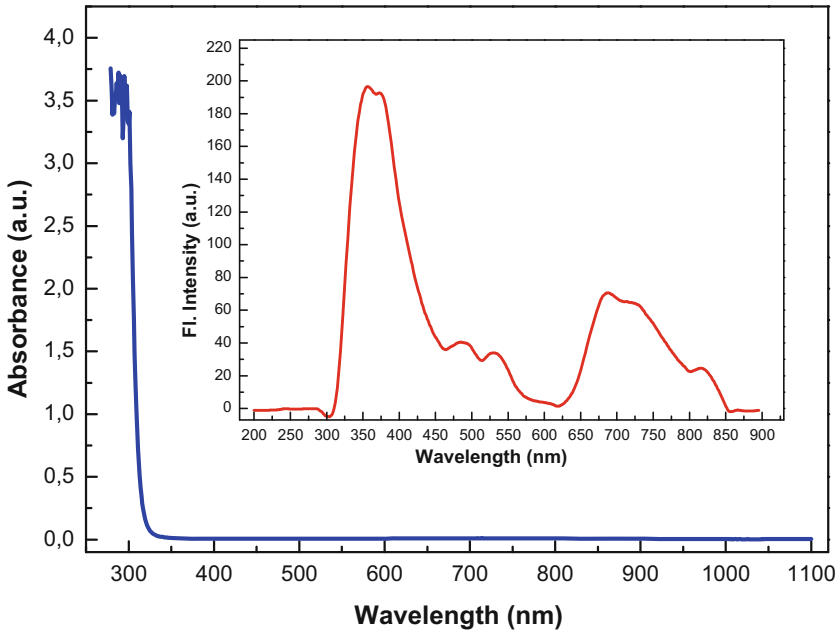

Fig. 5 Linear absorption spectra of the Zn(II) complex under room temperature conditions. Inset shows the emission spectra of the Zn(II) complex under 200 nm excitation

Conclusion

The bis(4-chlorophenylacetate)bis(4-pyridine carboxamide)zinc(II) was synthesized and characterized. The characterization of the complex was performed with elemental analysis, FT-IR spectroscopy and single crystal X-ray diffraction. The Zn^{II} cation is tetrahedrally coordinated by two oxygen atoms of the two 4-chlorophenylacetate anions and two nitrogen atoms from two 4-pyridine carboxamide ligands. The linear absorption spectra of the complex has been started to absorption edge around 321 nm wavelength and this corresponds to 3.86 eV in energy. Moreover, from the fluorescence spectra it was observed that the complex showed two emission peaks among 309–556 nm and 630–843 nm wavelengths. Therefore higher fluorescence intensity of emission peak was observed within the range of 309–556 nm wavelength, the synthesized complex can be used in the blue light OLED application by the filtering of the emission peak around 710 nm wavelength.

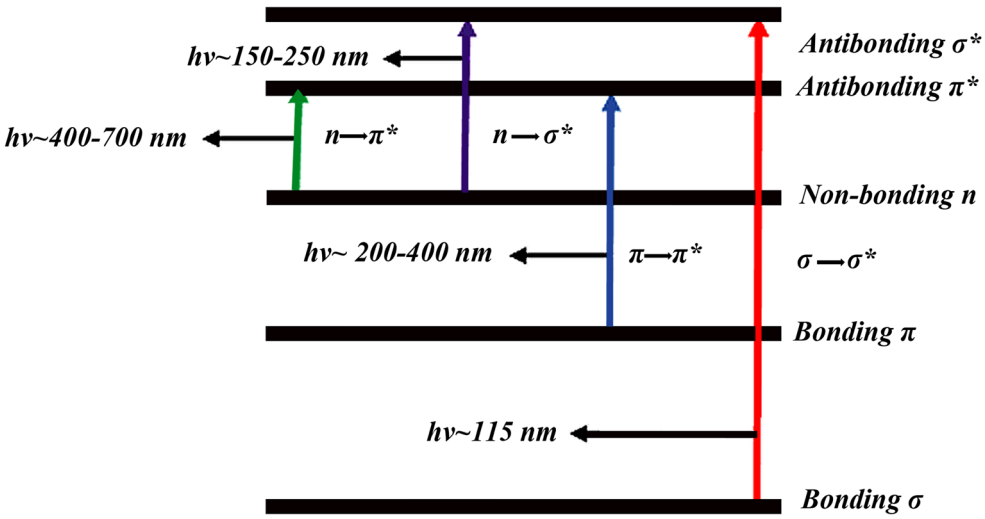

Fig. 6 Schematically demonstration of the electronic transitions, causing to the linear absorption behaviors in the organic complexes

Table 5 Electronic Energy, dipole moment (μ), polarizability (α) hyperpolarizability (β), the highest occupied and lowest unoccupied molecular orbital Energies (E_{HOMO} and E_{LUMO}) of the complex

B3LYP/6-31G						
Electronic Energy (a.u)	μ (D)	α (a.u)	β(a.u)	E_{HOMO} (a.u)	E_{LUMO} (a.u)	ΔEg (*eV*)
−1847.22588162	8.95	345,52	390.81	−0.238202	−0.101792	3712

Acknowledgements Crystallographic data for the structures 1 reported in this paper has been deposited with the Cambridge Crystallographic Data Center as supplementary publication No. CCDC-, 1905662. This work was supported by the Kafkas University Research Fund [Grant Number: 2015-FM-22].

Compliance with Ethical Standards

Conflict of Interest The authors declare that they have no conflict of interest.

References

1. Yaghi OM (2016) Reticular chemistry-construction, properties, and precision reactions of frameworks. J Am Chem Soc 138:15507–15509. https://doi.org/10.1021/jacs.6b11821
2. Tai X-S, Wang X (2015) Synthesis and crystal structure of a 1D chained coordination polymer constructed from Ca2+ and 2-[(E)-(2-Furoylhydrazono)methyl]benzenesulfonate. Crystals 5:458–465. https://doi.org/10.3390/cryst5040458
3. Liu S, Xu S, Wang J, Zhao F, Xia H, Wang Y (2017) Four-coordinate N-heterocyclic carbene (NHC) copper(I) complexes with brightly luminescence properties. J Coord Chem 70:584–599. https://doi.org/10.1080/00958972.2016.1278075
4. Hazari D, Jana SK, Puschmann H, Zangrando E, Dalai S (2015) Three new co-ordination polymers of zinc(II) and cadmium(II) with Dicarboxylate and Bipyridine ligands: synthesis, structure and luminescence study. J Inorg Organomet Polym Mater 25:1151–1159. https://doi.org/10.1007/s10904-015-0223-4
5. He J, Liu Z, Du G et al (2014) Chiral Palladium(II) and Nickel(II) complexes with C_2 -symmetrical tridentate Bis(oxazoline) ligands: synthesis, characterization, and catalytic norbornene polymerization. Organometallics 33:6103–6112. https://doi.org/10.1021/om5007616
6. Li-Hua W, Lei L, Xin W (2017) Synthesis, structural characterization and catalytic activity of a cu(II) coordination polymer constructed from 1,4-Phenylenediacetic acid and 2,2'-Bipyridine. Bull Chem React Eng Catal 12:113. https://doi.org/10.9767/bcrec.12.1.735.113-118
7. Lu F, Harms K (2017) Electrochemistry of dinuclear organometallic [5]Trovacenyl derivatives bridged by group 14 elements (Si, Ge, Sn, Pb): electrochemistry of Dinuclear organometallic [5]Trovacenyl derivatives bridged by group 14 elements (Si, Ge, Sn, Pb). Eur J Inorg Chem 2017:82–87. https://doi.org/10.1002/ejic.201601045
8. Cardoso JMS, Correia I, Galvão AM, Marques F, Carvalho MFNN (2017) Synthesis of ag(I) camphor sulphonylimine complexes and assessment of their cytotoxic properties against cisplatin -resistant A2780cisR and A2780 cell lines. J Inorg Biochem 166:55–63. https://doi.org/10.1016/j.jinorgbio.2016.11.003
9. Shang X, Ren K, Li J, Li W, Fu J, Zhang X, Zhang J (2017) Multi-properties of a cu(II) complex: crystal structure, anion binding ability, bioactivity and cell cytotoxicity. Inorganica Chim Acta 456:199–206. https://doi.org/10.1016/j.ica.2016.10.046
10. Liu W, Huang X, Xu C, Chen C, Yang L, Dou W, Chen W, Yang H, Liu W (2016) A multi-responsive regenerable europium-organic framework luminescent sensor for Fe^{3+} , Cr^{VI} anions, and picric acid. Chem Eur J 22:18769–18776. https://doi.org/10.1002/chem.201603607
11. Yang L-Z, Wang J, Kirillov AM, Dou W, Xu C, Fang R, Xu CL, Liu WS (2016) 2D lanthanide MOFs driven by a rigid 3,5-bis(3-carboxy-phenyl)pyridine building block: solvothermal syntheses, structural features, and photoluminescence and sensing properties. CrystEngComm 18:6425–6436. https://doi.org/10.1039/C6CE00885B
12. Barberis VP, Mikroyannidis JA (2006) Synthesis and optical properties of aluminum and zinc quinolates through styryl subsituent in 2-position. Synth Met 156:865–871. https://doi.org/10.1016/j.synthmet.2006.05.007
13. Lipunova GN, Nosova EV, Trashakhova TV, Charushin VN (2011) Azinylarylethenes: synthesis and photophysical and photochemical properties. Russ Chem Rev 80:1115–1133. https://doi.org/10.1070/RC2011v080n11ABEH004234
14. Wang S-L, Lin J-M (2007) Photophysics and applications in biosensor for 4′-N,N-dimethylamino-2-trans-styryl-(6-chloroquinoline). Chem Phys Lett 444:71–75. https://doi.org/10.1016/j.cplett.2007.06.122
15. Yüksek M, Elmali A, Durmuş M, Gul Yaglioglu H, Ünver H, Nyokong T (2010) Good optical limiting performance of indium and gallium phthalocyanines in a solution and co-polymer host. J Opt 12:015208. https://doi.org/10.1088/2040-8978/12/1/015208
16. Shirk JS, Pong RGS, Flom SR, Heckmann H, Hanack M (2000) Effect of axial substitution on the optical limiting properties of indium Phthalocyanines. J Phys Chem A 104:1438–1449. https://doi.org/10.1021/jp993254j
17. Hughes S, Spruce G, Wherrett BS, Kobayashi T (1997) Comparison between the optical limiting behavior of chloroaluminum phthalocyanine and a cyanine dye. J Appl Phys 81:5905–5912. https://doi.org/10.1063/1.364377
18. Yoon M, Moon D (2015) New Zr (IV) based metal-organic framework comprising a sulfur-containing ligand: enhancement of CO2 and H2 storage capacity. Microporous Mesoporous Mater 215:116–122. https://doi.org/10.1016/j.micromeso.2015.05.030
19. Venkatramaiah N, Kumar S, Patil S (2012) Fluoranthene based fluorescent chemosensors for detection of explosive nitroaromatics. Chem Commun 48:5007–5009. https://doi.org/10.1039/c2cc31606d
20. Lakowicz JR (2006) Principles of fluorescence spectroscopy. Springer US, Boston, MA
21. Iqbal M, Ali S, Tahir MN, Shah NA (2017) Dihydroxo-bridged dimeric cu(II) system containing sandwiched non-coordinating phenylacetate anion: crystal structure, spectroscopic, anti-bacterial, anti-fungal and DNA-binding studies of [(phen)(H 2 O)cu(OH) 2 cu(H 2 O)(phen)]2L.6H 2 O: (HL = phenylacetic acid; phen = 1,10-phenanthroline). J Mol Struct 1143:23–30. https://doi.org/10.1016/j.molstruc.2017.04.084

22. Chakrabarty PP, Biswas D, García-Granda S, Jana AD, Saha S (2012) Sodium ion assisted molecular self-assembly in a class of Schiff-base copper(II) complexes. Polyhedron 35:108–115. https://doi.org/10.1016/j.poly.2012.01.004
23. Deacon G (1980) Relationships between the carbon-oxygen stretching frequencies of carboxylato complexes and the type of carboxylate coordination. Coord Chem Rev 33:227–250. https://doi.org/10.1016/S0010-8545(00)80455-5
24. Wu WP, Wang J, Lu L, Wu Y (2016) Syntheses and luminescence of four supramolecular coordination complexes with flexible ligand. Russ J Coord Chem 42:217–224. https://doi.org/10.1134/S107032841603009X
25. Wen L, Yin H, Li W, Wang D (2010) New organoantimony complexes with the isomers of chlorophenylacetic acid: syntheses, characterizations and crystal structures of 1D polymeric chain, 2D network structure and 3D framework. Inorganica Chim Acta 363:676–684. https://doi.org/10.1016/j.ica.2009.11.022
26. Huang X, Sun H, Dou J, Li D, Wang D, Liu G (2007) A dimeric luminescent lanthanide complex $[Eu(PAA)_2(phen)(NO_3)]_2$: hydrothermal synthesis, crystal structure and fluorescence. J Coord Chem 60:2045–2050. https://doi.org/10.1080/00958970701236719
27. Sheng G-H, Cheng X-S, You Z-L, Zhu H-L (2015) Syntheses, crystal structures, and characterization of copper(II) and zinc(II) complexes derived from N,N-Dimethylethane-1,2-diamine and Phenylacetic acid derivatives. Synth React Inorg Met-Org Nano-Met Chem 45:1273–1277. https://doi.org/10.1080/15533174.2013.862697
28. Zhang W-M, Li M-H, Sun J, Lv PC, Zhu HL (2014) Synthesis, characterization, and antibacterial evaluation of copper(II) complexes supported by phenylacetic acid derivatives, and diamine ligands. J Coord Chem 67:3519–3531. https://doi.org/10.1080/00958972.2014.976563
29. Iqbal M, Ahmad I, Ali S, Muhammad N, Ahmed S, Sohail M (2013) Dimeric "paddle-wheel" carboxylates of copper(II): synthesis, crystal structure and electrochemical studies. Polyhedron 50:524–531. https://doi.org/10.1016/j.poly.2012.11.037
30. Ahuja IS, Prasad I (1976) Isonicotinamide complexes with some metal(II) halides and pseudohalides. Inorg Nucl Chem Lett 12:777–784. https://doi.org/10.1016/0020-1650(76)80065-7
31. Homzová K, Györyová K, Koman M, Melník M, Juhászová Ž (2015) Synthesis, crystal structure, and spectroscopic and thermal properties of the polymeric compound *catena* -poly[[bis(2,4-dichlorobenzoato)zinc(II)]-μ-isonicotinamide]. Acta Crystallogr Sect C Struct Chem 71:814–819. https://doi.org/10.1107/S2053229615014862
32. Hökelek T, Dal H, Tercan B, Özbek FE, Necefoğlu H (2009) Tetraaquabis(nicotinamide-κ N^1)nickel(II) bis(2-fluorobenzoate). Acta Crystallogr Sect E Struct Rep Online 65:m1330–m1331. https://doi.org/10.1107/S1600536809040392
33. Özbek FE, Yüksek M, Necefoğlu H (2016) Synthesis, spectroscopic and fluorescence properties of N , N ′-diethylnicotinamide adducts of 2-bromobenzoate co(II) and Ni(II) metal-organic complexes. Opt - Int J Light Electron Opt 127:7710–7716. https://doi.org/10.1016/j.ijleo.2016.05.138
34. Özbek FE, Sertçelik M, Yüksek M, Küçüköz B, Elmali A, Şahin E (2019) Two new potential optical materials: co(II) and Ni(II) 3-fluorobenzoate complexes with pyridine-3-carboxamide. J Coord Chem 72:786–795. https://doi.org/10.1080/00958972.2019.1590560
35. Sheldrick GM (2008) A short history of *SHELX*. Acta Crystallogr A 64:112–122. https://doi.org/10.1107/S0108767307043930
36. Lee C, Yang W, Parr RG (1988) Development of the Colle-Salvetti correlation-energy formula into a functional of the electron density. Phys Rev B 37:785–789. https://doi.org/10.1103/PhysRevB.37.785
37. Becke AD (1993) Density-functional thermochemistry. III. The role of exact exchange. J Chem Phys 98:5648–5652. https://doi.org/10.1063/1.464913
38. Hehre WJ (1986) Ab initio molecular orbital theory. Wiley, New York
39. Frisch M, Trucks G, Schlegel H, et al (2009) Gaussian 09, Revision B.01. Gaussian 09 Revis B01 Gaussian Inc Wallingford CT
40. Dennington R, Keith T, Millam J (2009) GaussView, Version 5.0.8. Semichem Inc., Shawnee Mission KS http://www.oalib.com/references/12626365. Accessed 15 Mar 2019
41. Bernstein J, Davis RE, Shimoni L, Chang N-L (1995) Patterns in hydrogen bonding: functionality and graph set analysis in crystals. Angew Chem Int Ed Engl 34:1555–1573. https://doi.org/10.1002/anie.199515551
42. Pavia DL, Lampman GM, Kriz GS (2001) Introduction to spectroscopy: a guide for students of organic chemistry, 3rd edn. Brooks/Cole, South Melbourne
43. Nakamoto K (2008) Infrared and Raman spectra of inorganic and coordination compounds. John Wiley & Sons, Inc., Hoboken, NJ, USA
44. Kaya AA, Demircioğlu Z, Kaya EÇ, Büyükgüngör O (2014) Synthesis, X-ray structural characterization, NLO, MEP, NBO and HOMO-LUMO analysis using DFT study of Zn(II)bis(3,4 dimethoxybenzoate)bis(nicotinamide) dihydrate. Heterocycl Commun 20. https://doi.org/10.1515/hc-2013-0160
45. Zhan C-G, Nichols JA, Dixon DA (2003) Ionization potential, Electron affinity, electronegativity, hardness, and Electron excitation energy: molecular properties from density functional theory orbital energies. J Phys Chem A 107:4184–4195. https://doi.org/10.1021/jp0225774
46. Yüksek M, Elmali A, Karabulut M, Mamedov GM (2010) Nonlinear absorption in undoped and Ge doped layered GaSe semiconductor crystals. Appl Phys B Lasers Opt 98:77–81. https://doi.org/10.1007/s00340-009-3665-y
47. Wang L, Li X-Y, Zhao Q, Li LH, Dong WK (2017) Fluorescence properties of heterotrinuclear Zn(Ⅱ)–M(Ⅱ) (M = ca, Sr and Ba) bis(Salamo)-type complexes. RSC Adv 7:48730–48737. https://doi.org/10.1039/C7RA08789F
48. Zhang Y-C (2017) Synthesis, crystal structure, and fluorescent property of a Zn(II) complex with N-Nicotinoylglycine ligand. Crystals 7:151. https://doi.org/10.3390/cryst7060151
49. Kamath A, Netalkar SP, Gangaram Kokare D, Naik K, Revankar VK (2012) Phenoxide bridged tetranuclear co(II), Ni(II), cu(II) and Zn(II) complexes: syntheses, characterization and fluorescence studies. J Lumin 132:2763–2768. https://doi.org/10.1016/j.jlumin.2012.05.025
50. Zhao F, Ma X, Meng Y, Ge J, Jin H, Liu S, Zhan L, Zhu M, Gao E (2016) Synthesis, structure, DNA binding, and cleavage of a Zn(II) complex constructed by 4,4'-Bipyridine and Phenylacetic acid. Synth React Inorg Met-Org Nano-Met Chem 46:1041–1046. https://doi.org/10.1080/15533174.2015.1004415
51. Shit S, Chakraborty J, Samanta B, Rosair GM, Mitra S (2009) Synthesis, structure and fluorescence properties of a Trinuclear Zn(II) complex with N,N,O-donor Schiff Base ligands and bridging acetates. Z Für Naturforschung B 64:403–408. https://doi.org/10.1515/znb-2009-0408
52. Ray A, Banerjee S, Sen S, Butcher RJ, Rosair GM, Garland MT, Mitra S (2008) Two Zn(II) and one Mn(II) complexes using two different hydrazone ligands: spectroscopic studies and structural aspects. Struct Chem 19:209–217. https://doi.org/10.1007/s11224-007-9274-7
53. Majumder A, Shit S, Choudhury CR, Batten SR, Pilet G, Luneau D, Daro N, Sutter JP, Chattopadhyay N, Mitra S (2005) Synthesis, structure and fluorescence of two novel manganese(II) and zinc(II)-1,3,5-benzene tricarboxylate coordination polymers: extended 3D supramolecular architectures stabilised by hydrogen

bonding. Inorganica Chim Acta 358:3855–3864. https://doi.org/10.1016/j.ica.2005.07.002

54. Liu H, Yao L, Li B, Chen X, Gao Y, Zhang S, Li W, Lu P, Yang B, Ma Y (2016) Excimer-induced high-efficiency fluorescence due to pairwise anthracene stacking in a crystal with long lifetime. Chem Commun 52:7356–7359. https://doi.org/10.1039/C6CC01993E
55. Wang W-J, Hao L, Chen C-Y, Qiu QM, Wang K, Song JB, Li H (2017) Red-shift in fluorescence emission of D–A type asymmetrical Zn(II) complexes by extending the π–π stacking interaction. RSC Adv 7:20488–20493. https://doi.org/10.1039/C7RA01135K